

ORIGINAL ARTICLE

Exogenous rhTRX reduces lipid accumulation under LPS-induced inflammation

Gi-Yeon Han, Eun-Kyung Lee, Hey-won Park, Hyun-Jung Kim and Chan-Wha Kim

Redox-regulating molecule, recombinant human thioredoxin (rhTRX) which shows anti-inflammatory, and anti-oxidative effects against lipopolysaccharide (LPS)-stimulated inflammation and regulate protein expression levels. LPS-induced reactive oxygen intermediates (ROI) and NO production were inhibited by exogenous rhTRX. We identified up/downregulated intracellular proteins under the LPS-treated condition in exogenous rhTRX-treated A375 cells compared with non-LPS-treated cells via 2-DE proteomic analysis. Also, we quantitatively measured cytokines of *in vivo* mouse inflammation models using cytometry bead array. Exogenous rhTRX inhibited LPS-stimulated production of ROI and NO levels. TIP47 and ATP synthase may influence the inflammation-related lipid accumulation by affecting lipid metabolism. The modulation of skin redox environments during inflammation is most likely to prevent alterations in lipid metabolism through upregulation of TIP47 and ATP synthase and downregulation of inflammatory cytokines. Our results demonstrate that exogenous rhTRX has anti-inflammatory properties and intracellular regulatory activity *in vivo* and *in vitro*. Monitoring of LPS-stimulated pro-inflammatory conditions treated with rhTRX in A375 cells could be useful for diagnosis and follow-up of inflammation reduction related with candidate proteins. These results have a therapeutic role in skin inflammation therapy.

Experimental & Molecular Medicine (2014) 46, e71; doi:10.1038/emm.2013.136; published online 10 January 2014

Keywords: inflammation; lipid accumulation; rhTRX; skin cell proteomics; TIP47

INTRODUCTION

Skin, the largest organ of the human body, is the most important interface between the environment and the body. It is constantly exposed to chemical and physical environmental pollutants or their metabolic toxicants, which are associated with a wide range of inflammatory skin diseases. Inflammatory skin diseases, such as dermatitis, systemic inflammatory response syndrome (SIRS) and sepsis, are known to affect the whole body, which results in systemic inflammation, organ dysfunction and organ failure.¹ Recent studies have reported that oxidative stress has a critical role in the upregulation of local inflammatory mediators.² Moreover, severe depletion of antioxidants in the skin caused by prolonged exposure to reactive oxygen species (ROS) results in insufficient protection, triggering cellular damage.^{3–6} Thus, reactive oxygen intermediates (ROI) have emerged as promising targets for anti-inflammatory drug discovery. Topical application or oral administration of antioxidants has been suggested as an effective preventive therapy for inflammatory skin diseases.

Thioredoxin (TRX) is a multifunctional thiol molecule with antioxidant, anti-inflammatory and antiapoptotic properties.^{7,8}

It functions as a general oxidoreductase with a conserved CXXC active site that forms a disulfide in the oxidized form and a dithiol in the reduced form.^{9–12} These two cysteines are the key for the ability of TRX to facilitate the reduction of other proteins and maintain cellular redox homeostasis.^{13–18} TRX levels have been shown to be related with organism lifespan and age-associated tissue deterioration.¹⁸ Recent studies have reported that TRX has protective effects against various inflammatory diseases.² In addition, TRX expression is enhanced under various inflammatory conditions.^{8,19} TRX treatment decreases not only oxidative stress but also the inflammatory mediator NO.²⁰ Accumulated evidence has also suggested that the administration of recombinant redox-regulating molecule recombinant human thioredoxin (rhTRX) induces increased tolerance against oxidative stress and inflammation.^{21,22} However, despite recent progress in TRX research in terms of inflammation, the protective effects and action mechanisms against skin inflammation have not yet been entirely elucidated. Therefore, this study was conducted to evaluate the protective effects of exogenous rhTRX on LPS-stimulated skin cells. To determine this, we used proteomic techniques in the belief that large-scale analyses

via proteomic approaches might help to systematically understand the action mechanisms of rhTRX on inflammatory skin diseases. In addition, as a skin inflammation model, the human melanocyte cell line, A375 melanoma, as well as C57BL/6 mice, was used. As only a few studies have examined this phenomenon, the results of this study would also help broaden our understanding of inflammatory damage in melanocytes. Here we report that exogenous rhTRX regulates inflammatory skin conditions, especially through its ability to modulate lipid metabolism by prompting the expression of related proteins TIP47 and ATP synthase and by decreasing TNF- α , MCP-1 and IL-6. Elucidation of the mechanism underlying the anti-inflammatory function of exogenous rhTRX might contribute to the discovery of new therapeutic targets for the treatment of skin inflammation-related diseases.

MATERIALS AND METHODS

Purification of rhTRX

rhTRX was purified from *Escherichia coli* BL21 (DE3) pLysS transformed with pET28a-6His-rhTRX. The expression vector encoded the full-length rhTRX protein, which is nearly identical to the human TRX-1, fused to a polyhistidine tag at its NH₂ terminus. Protein expression and purification were conducted under native conditions using Ni-NTA resin (Qiagen, Valencia, CA, USA) following the manufacturer's recommendations. Residual RNA and DNA were removed from the column by incubating the resin with a buffer containing 50 mM of NaH₂PO₄, 300 mM of NaCl, 10 mM of imidazole, 10 mM of β -mercaptoethanol, pH 8.0, DNase (Promega, Madison, WI, USA; 1.5 μ g ml⁻¹) and RNase A (15 μ g ml⁻¹) for 2 h at 25 °C with continuous shaking. rhTRX was then eluted with a buffer containing 50 mM of NaH₂PO₄, 300 mM of NaCl, 50 mM of imidazole and 10 mM of β -mercaptoethanol, pH 8.0. Residual bacterial LPS was extracted using Triton X-114. Briefly, 1/20 (v/v) Triton X-114 was added to the solution containing the recombinant protein. The mixture was incubated for 1 h at 4 °C with constant rotation for 20 min at 37 °C. The sample was then centrifuged at 4500 g for 15 min. The supernatant was collected and extensively dialyzed against PBS. Residual bacterial LPS was measured with the E-toxate reagent (Sigma, St Louis, MO, USA) according to the manufacturer's instructions.²³

Cell culture and reagents

The human melanoma cell line A375 melanoma was purchased from the American Type Culture Collection (Rockville, MA, USA, CRL-1619). A375 cells were cultivated at 37 °C in a humidified incubator supplied with 5% CO₂. The medium consisted of DMEM supplemented with 10% of fetal bovine serum, penicillin (100 U ml⁻¹) and streptomycin (100 μ g ml⁻¹). When the A375 cells were 80% confluent, they were treated with bacterial LPS (10 μ g ml⁻¹). Medium and other cell culture reagents were obtained from Gibco-BRL (Grand Island, NE, USA). Precast IPG strips and other reagents used in 2-DE experiments were from Amersham Biosciences (Uppsala, Sweden). Antibodies were from Santa Cruz Biotechnology (Santa Cruz, CA, USA).

Detection of ROIs and NO

Intracellular ROI production was measured by following the method described by Hyun *et al.*²⁴ Briefly, A375 melanoma cells (1 \times 10⁴ cells/

well) were placed in a 96-well plate and activated with 10 μ g ml⁻¹ of bacterial LPS (*E. coli* serotype 0111:B4; Sigma). After 4 h, the cells were treated with exogenous rhTRX and then incubated with 50 μ M of 2', 7'-dichlorodihydrofluorescein diacetate (DCFH-DA; Sigma). ROI generation was analyzed using a Multilabel Plate Reader (Perkin Elmer, MA, USA) with excitation at 485 nm and emission at 530 nm.

Nitrite formation was determined using the Griess assay according to the manufacturer's instructions (Promega, Heidelberg, Germany). A375 melanoma cells were seeded at a density of 1 \times 10⁵ cells per well in 96-well plates. After incubation for 12 h, cells were incubated with 10 μ g ml⁻¹ of LPS for 4 h. Thereafter, medium was changed and the cells were further incubated for 4 h with or without the addition of 50 μ g ml⁻¹ of rhTRX. Nitrite concentrations in the supernatant of A375 melanoma cells were calculated in comparison with standard concentrations of NaNO₂ dissolved in culture medium or PBS. Absorbance was read at 540 nm, and nitrite concentrations were calculated.

2-DE and image analysis

2-DE samples were prepared according to the previously described methods.²⁵⁻²⁹ After delipidation and desalting, the protein concentration of the samples was measured via a modified Bradford method using BSA as a standard.³⁰ Immobilized DryStrips (24 cm, pH 3-10) utilized for isoelectric focusing (IEF) were rehydrated with 40 μ g of protein in 450 μ l of solubilization solution containing 8 M of urea, 2% of CHAPS, 1% of immobilized pH gradient (IPG) buffer (pH 3-10), 13 mM of dithiothreitol (DTT) and a trace of bromophenol blue for 5 h without current and for another 7 h at 80 V. IEF was conducted using the IPGphor IEF system (GE Healthcare, Uppsala, Sweden) for 120 000 Vhr. The second dimension was run on 12.5% of SDS-PAGE with an Ettan DALT II system (GE Healthcare). Proteins were visualized *via* silver staining. All experiments were conducted in triplicate. Computer analyses of the 2-DE images were conducted using an ImageMaster 2D Elite Software (GE Healthcare). The expression levels of the spots were determined in accordance with the relative spot volume of each protein, as compared with the normalized volumes of proteins.³¹

Protein identification by ESI Q-TOF MS/MS

Excised gel spots were destained using 100 μ l of destaining solution (1:1 = 30 mM potassium ferricyanide: 100 mM sodium thiosulfate, v/v) for 5 min with agitation. After removal of the solution, the gel spots were incubated for 20 min with 200 mM of ammonium bicarbonate. The gel pieces were then dehydrated with 100 μ l of acetonitrile and dried in a vacuum centrifuge. The dried gel pieces were rehydrated with 20 μ l of 50 mM ammonium bicarbonate containing 0.2 μ g of modified trypsin (Promega Corp., WI, USA) on ice for 45 min. After the removal of the solution, 30 μ l of 50 mM ammonium bicarbonate was added. The digestion was performed overnight at 37 °C. The peptide solution was desalted using a ZipTip_{C18} nano column (Millipore Corp., Bedford, MA, USA). Thirty microliters of the peptide mixture from the digestion supernatant was diluted in 30 μ l of 5% formic acid, loaded onto the column and then washed with 30 μ l of 5% formic acid. For MS/MS analysis, the peptides were eluted with 1.5 μ l of 50% methanol, 49% H₂O and 1% formic acid directly into a precoated borosilicate nanoelectrospray needle (Micromass, Manchester, UK).

MS/MS of the peptides generated by in-gel digestion was conducted *via* nano-ESI on a Q-TOF2 mass spectrometer (Micromass). The product ions were analyzed with an orthogonal TOF analyzer

equipped with a reflector, a micro-channel plate detector and a time-to-digital converter. The data were then processed using a Mass Lynx Windows NT PC system (Micromass). All MS/MS spectra recorded on tryptic peptides derived from spots were searched against protein sequences from NCBI databases using the MASCOT search program (version 2.1 Matrix Science, Boston, MA, USA). The non-redundant database NCBI from NCBI is a frequently used protein database for protein identification.

In vivo mouse model and cytometric bead array

C57BL/6 mice were purchased from Orient BIO (Sung-nam, Korea) and maintained in laboratory animal facilities. Six-week-old inbred female mice were used for the experiments. The animal experiments were performed in accordance with the NIH guidelines (USA) for laboratory animal use and care. Inflammation was induced by subcutaneous injection of $100\ \mu\text{g ml}^{-1}$ of LPS (*E. coli* serotype 0111:B4; Sigma). The LPS-stimulated mice were treated with 20 μg , 40 μg or 80 μg of rhTRX by subcutaneous injection.

Using a CBA kit (BD Biosciences, San Diego, CA, USA), the levels of IL-6, IL-10, MCP-1, IFN- γ , TNF- α and IL-12 were quantitatively measured from serum. The results were analyzed with a BD CBA analysis software (BD Biosciences).^{32,33} Control mice received sterile PBS, and five mice were used for each data point ($n = 5$).

Oil Red O staining

Cryosections on glass slides were fixed with 10% (v/v) formaldehyde in PBS for 1 h at 23 °C, rinsed twice with water and then stained with 0.1% (w/v) Oil Red O in 75% (v/v) isopropanol at 23 °C. After 2 h, the stained cryosections on glass slides were rinsed twice with water to remove unincorporated dye and photographed using a Zeiss AxioVert microscope with phase contrast optics and Hamamatsu digital/video camera.

Statistical analysis

All data were expressed as means \pm s.d. Statistical comparisons were made using Student's *t* test or ANOVA coupled with a Fisher's test. A statistically significant difference was defined as $P < 0.05$, which is represented by an asterisk in the data presentation.

RESULTS

TRX inhibits LPS-stimulated production of ROI and NO

Effects of TRX on oxidative stress and inflammation in skin were investigated by examining the ROI and NO levels in A375 melanoma cells treated with or without rhTRX after exposure to LPS. First, to examine whether rhTRX influences ROI levels, A375 melanoma cells were incubated in medium containing various concentrations of LPS for 4 h followed by incubation with or without $50\ \mu\text{g ml}^{-1}$ of rhTRX. After 4 h, the intracellular ROI level was quantified using a fluorescein derivative DCFH-DA as a redox indicator. A LPS concentration-dependent increase of intracellular ROI was observed in A375 melanoma cells (Figure 1a). In contrast, in cells treated with rhTRX, the increased intracellular ROI level following LPS stimulation decreased, which indicates that exogenous rhTRX treatment diminished the oxidative stress.

LPS also remarkably increased NO production in A375 melanoma cells, which was greatly decreased by rhTRX

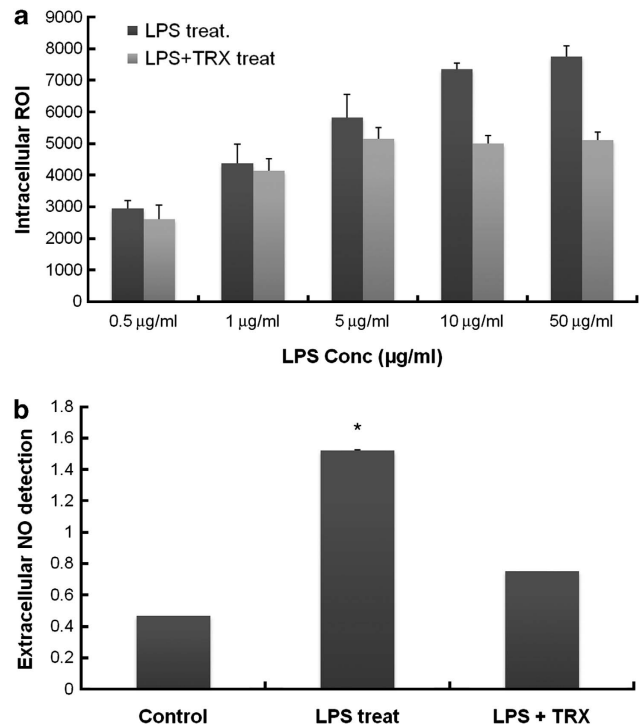


Figure 1 Effect of exogenous rhTRX on production of ROI and NO in LPS-stimulated A375 melanoma cells. **(a)** A375 melanoma cells (3×10^5 per ml) were incubated in medium containing various concentrations of LPS for 4 h and then administered with or without $50\ \mu\text{g ml}^{-1}$ of rhTRX. After 4 h, the cells were collected, washed with PBS and treated with $50\ \mu\text{M}$ of DCFH-DA. The ROI levels were measured using flow cytometry. Data represent the mean \pm s.d. **(b)** A375 melanoma cells (3×10^5 per ml) were stimulated with $10\ \mu\text{g ml}^{-1}$ of LPS for 4 h and then treated with or without $50\ \mu\text{g ml}^{-1}$ of rhTRX. After 4 h, the nitrite concentration was determined in the supernatant fluid using the Griess assay. The Griess assay data represent the s.e.m. of at least three different experiments ($*P \leq 0.05$ vs controls).

(Figure 1b). The NO level produced from cells exposed to $10\ \mu\text{g ml}^{-1}$ of LPS for 4 h was 3.25-fold higher than that from control cells. However, treatment with $50\ \mu\text{g ml}^{-1}$ of rhTRX for another 4 h reduced the LPS-stimulated increase in NO by 2.03-fold, which demonstrates the protective effects of rhTRX against inflammation. Taken together, TRX might protect melanocytes from oxidative stress and inflammation-induced damage by attenuating the LPS-stimulated production of ROI and NO.

TRX attenuates LPS-stimulated changes in protein expression

As exogenous rhTRX treatment reduced the LPS-stimulated production of ROI and NO (Figure 1), it was highly possible that this treatment affected expression of proteins related to oxidative stress and inflammation. To systematically determine this, we used proteomic techniques. Proteomes in A375 melanoma cells exposed to $10\ \mu\text{g ml}^{-1}$ of LPS for 4 h followed by treatment with or without $50\ \mu\text{g ml}^{-1}$ of rhTRX for 4 h

were analyzed using the two-dimensional electrophoresis (2-DE) and compared with in the proteomes of control cells. two-dimensional electrophoresis analysis revealed that exposure of A375 melanoma cells to LPS with or without TRX resulted in marked changes in protein levels compared with control cells (Figure 2a). Among the proteins visualized on the 2-DE gels, 14 spots that were significantly up or down-regulated, which showed either 50% downregulation or 100% upregulation compared with those of control cells within the 95% significance level, were selected for identification *via* ESI Q-TOF MS/MS (Tables 1 and 2). Table 1 shows two upregulated and four downregulated proteins in LPS-stimulated A375 melanoma cells, compared with control cells. The upregulated proteins were identified as pyrophosphatase

and ubiquitin carboxyl-terminal esterase. The downregulated proteins were cargo selection protein TIP47, prohibitin, ATP synthase and TRX. Table 2 shows five upregulated and three downregulated proteins in A375 melanoma cells stimulated with LPS and then treated with rhTRX, compared with control cells. The differentially expressed proteins included pyrophosphatase, ubiquitin carboxyl-terminal esterase, pyrophosphatase, heterogeneous nuclear ribonucleoprotein and nuclear chloride channel.

Of the proteins that were differentially expressed by LPS stimulation, exogenous rhTRX significantly reduced the LPS-stimulated changes in the protein expression of cargo selection protein TIP47, ATP synthase and TRX (Figure 2b). Exposure of A375 melanoma cells to LPS resulted in distinctly decreased

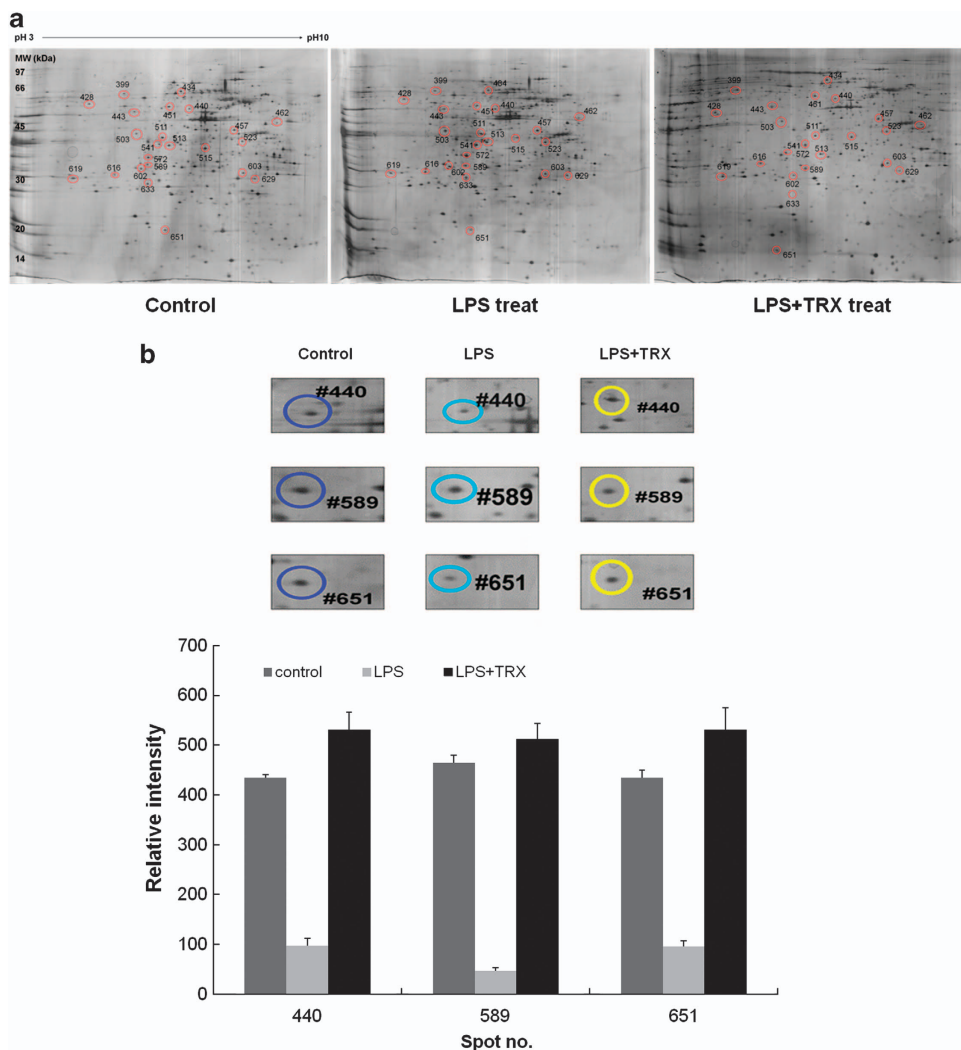


Figure 2 Proteomic analysis of A375 melanoma cells exposed to LPS and then treated with or without rhTRX. A375 melanoma cells were exposed to $10\mu\text{gml}^{-1}$ of LPS for 4 h and subsequently treated with or without $50\mu\text{gml}^{-1}$ of rhTRX for 4 h. Proteins ($50\mu\text{g}$) were separated by IEF using 24 cm, pH 3–10 IPG strips and 12.5% homogenous SDS–PAGE. The gels were visualized with silver staining, and their maps were analyzed with an Image Master 2D Elite Software (GE Healthcare, Sweden). **(a)** Representative 2-DE maps. **(b)** Magnified 2-DE maps and relative volume intensity of three differentially expressed spots between A375 melanoma cells treated with or without rhTRX after LPS stimulation. The three proteins were identified as TIP47 (#440), ATP synthase (#589) and thioredoxin (#651) by ESI Q-TOF MS/MS.

Table 1 Identification of the up- and downregulated proteins in LPS-stimulated A375 melanoma cells compared with control A375 melanoma cells using ESI Q-TOF MS/MS

Spot No.	Protein identification	Accession No. (gi)	MW (Da)	pI	MOWSE score ^a	Queries matched	Sequence coverage (%)	Up/Down
541	Pyrophosphatase 1	gil11056044	33 095	5.54	148	3	11	Up
629	Ubiquitin carboxyl-terminal esterase L3	gil5174741	26 337	4.84	192	3	22	Up
440	Cargo selection protein	gil3095186	47 175	5.3	327	7	14	Down
513	Prohibitin	gil4505773	29 843	5.57	408	7	29	Down
589	ATP synthase, H ⁺ transporting, mitochondrial FO complex, subunit d isoform a	gil5453559	18 537	5.21	57	1	10	Down
651	Thioredoxin-like 5	gil14249348	14 217	5.4	216	4	46	Down

^aScore is $-10 \times \log(P)$, where P is the absolute probability that the observed match between the experimental data and the database sequence is a random event. The NCBI nr database is used through MASCOT searching program (<http://www.matrixscience.com/>) with ESI-Q-TOF MS/MS data as an input.

Table 2 Identification of the up- and down-regulated proteins in LPS-stimulated A375 melanoma cells treated with exogenous rhTRX compared with control A375 melanoma cells using ESI Q-TOF MS/MS

Spot No.	Protein identification	Accession no. (gi)	MW (Da)	pI	MOWSE score ^a	Queries matched	Sequence coverage (%)	Up/Down
381	Zinc-finger protein 259	gil4508021	51 463	4.66	108	3	9	Up
541	Pyrophosphatase 1	gil11056044	33 095	5.54	148	3	11	Up
608	Nm23 protein	gil35068	20 740	7.07	185	5	33	Up
619	Ribosomal protein P2	gil4506671	11 658	4.42	213	5	69	Up
629	Ubiquitin carboxyl-terminal esterase L3	gil5174741	26 337	4.84	192	3	22	Up
385	Pyrophosphatase 1	gil11056044	33 095	5.54	148	3	11	Down
434	Heterogeneous nuclear ribonucleoprotein K transcript variant	gil59381084	51 312	5.19	183	5	20	Down
511	Nuclear chloride channel	gil4588526	27 249	5.02	403	7	42	Down

^aScore is $-10 \times \log(P)$, where P is the absolute probability that the observed match between the experimental data and the database sequence is a random event. The NCBI nr database is used through MASCOT searching program (<http://www.matrixscience.com/>) with ESI-Q-TOF MS/MS data as an input.

levels of cargo selection protein TIP47, ATP synthase and TRX, which were completely restored to baseline levels by exogenous rhTRX. On the basis of the previous reports demonstrating that TIP47 and ATP are intimately associated with lipid metabolism,^{34–39} we concluded that TRX might exert its protective effects on LPS-mediated inflammation at least in part through its ability to modulate a lipid metabolism-dependent pathway by upregulating proteins related to this pathway, such as TIP47 and ATP synthase.

TRX reduces inflammation-induced lipid accumulation

The Oil Red O stain was used to confirm the results obtained from the 2-DE analysis, suggesting that the protective effects of TRX against inflammation-induced skin cell damage might involve inhibiting alterations in lipid metabolism. A subcutaneous injection of LPS significantly promoted lipid accumulation in the skin of C57BL/6 mice (Figure 3). However, exogenous rhTRX inhibited the effect of LPS in a concentration-dependent manner. As the rhTRX concentration was increased, Oil Red O-stained lipid droplets in the cytoplasm decreased gradually in LPS-injected mice. On the basis of the

results shown in Figures 2 and 3, we concluded that TRX protects against inflammation-induced skin cell damage by reducing lipid accumulation.

TRX decreases inflammatory cytokines

We determined whether skin cell damage after LPS stimulation involves inflammatory cytokines. In these experiments, rhTRX was shown to affect LPS-induced damage. As depicted in the cytometric bead array (CBA) results (Figure 4), inflammatory cytokines IL-6, MCP-1, IFN- γ and TNF- α were significantly increased in LPS-injected mice. However, rhTRX dose dependently reduced the secretion of the inflammatory cytokines stimulated by LPS. Levels of IL-10 and IL-12 were not changed in LPS-injected mice. In addition, mice treated with only rhTRX did not exhibit significant differences in the levels of cytokines examined, which indicates that the inactive network of exogenous rhTRX was rapidly activated in response to bacterial LPS. It should be noted that among the inflammatory cytokines, TNF- α , MCP-1 and IL-6 have also been reported to affect lipid metabolism. Therefore, we concluded that the anti-

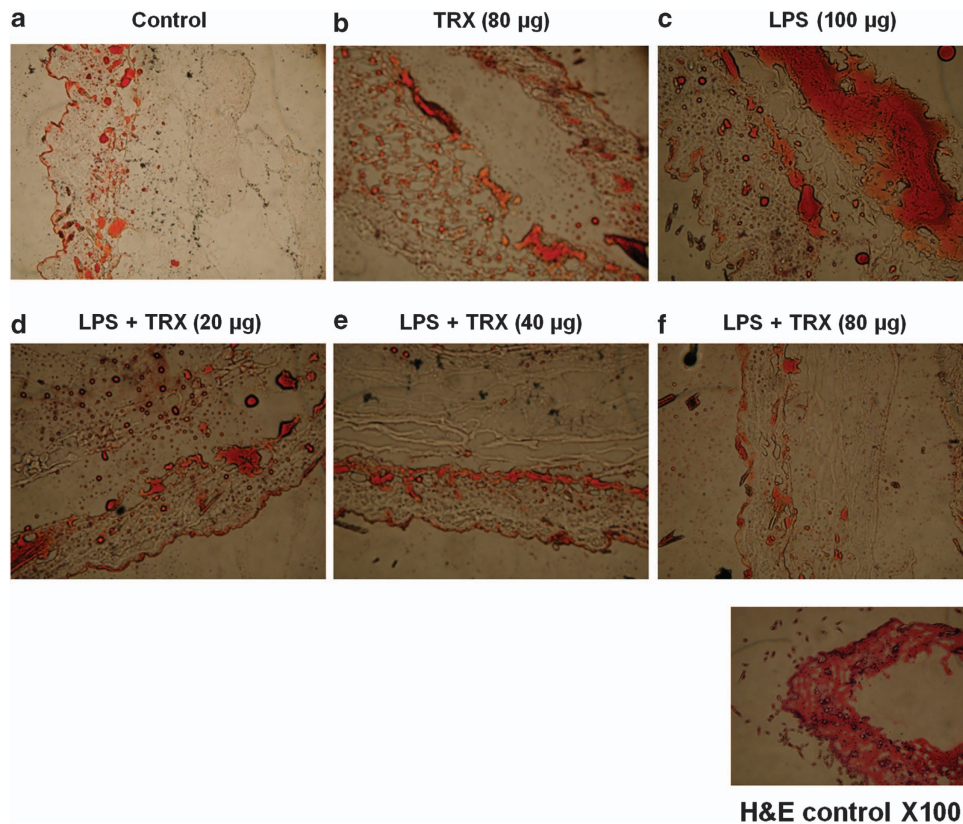


Figure 3 Effect of TRX on inflammation-induced lipid accumulation. C57BL/6 mice were subcutaneously injected with 100 µg of LPS and, after 4 h, with various concentrations of rhTRX. After another 4 h, cryostat sections of the skin were prepared and stained with Oil Red O. The LPS-stimulated mice were treated with 20 µg, 40 µg, or 80 µg of rhTRX by subcutaneous injection (a–f). Images were acquired at a magnification of $\times 100$.

inflammatory effects of TRX involve decreasing the levels of inflammatory cytokines that alter lipid metabolism.

DISCUSSION

TRX is an oxidoreductase that contains a dithiol–disulfide active site. Its two cysteines in a CXXC motif contribute to the function of TRX as an antioxidant.^{9–12} It has been reported that extracellular levels of TRX increase in response to oxidative stress and inflammation,^{8,19} which indicates the direct involvement of TRX in cellular defense systems. This study also demonstrates the protective effects of TRX against oxidative stress and inflammation by showing that exogenous rhTRX decreased the LPS-stimulated production of ROI and NO in A375 melanoma cells (Figure 1).

After demonstrating that exogenous rhTRX alleviated the inflammation induced by bacterial LPS, it was necessary to identify the proteins associated with this effect, as these proteins could become potential targets for inflammatory studies and drug development. Proteomic analysis was performed to evaluate the protection mechanism of TRX against inflammation-induced skin damage. In these experiments, TRX was found to not only decrease LPS-stimulated production of ROI and NO in A375 melanoma cells but also reduce LPS-induced changes in protein expression (Tables 1 and 2, and Figure 2). In particular, of the differentially expressed

proteins by LPS stimulation, exogenous rhTRX significantly attenuated LPS-induced downregulation of cargo selection protein TIP47, ATP synthase and TRX. This suggests a potential link between the ability of TRX to decrease LPS-stimulated production of ROI and NO and its ability to stimulate the expression of three genes encoding cargo selection protein TIP47, ATP synthase and TRX under inflammatory conditions. Inflammation has been recognized as a central component in the pathogenesis of many life-threatening diseases.⁴⁰ One hallmark of inflammation is non-enzymatic oxidation of cellular lipids resulting in the formation of bioactive and toxic products, which modulates inflammation.^{40,41} An increase in the content of cellular lipids is also known to activate inflammation.⁴² Many studies reported that cellular inflammatory responses rely on diverse factors that determine lipid metabolism. Proteins of the PAT family, including perilipin, adipophilin and TIP47, have been recognized as critical regulators of lipid accumulation.⁴³ The PAT proteins are not only associated with lipid droplets but also directly involved in the biogenesis of lipid droplets.^{43,44} Further, they regulate lipid droplet turnover by modulating lipolysis. Recent studies have shown that downregulation of the PAT proteins results in abnormal lipid droplet metabolism and accumulation, which leads to the development of insulin resistance in obesity.⁴⁵ ATP synthase is also known to be

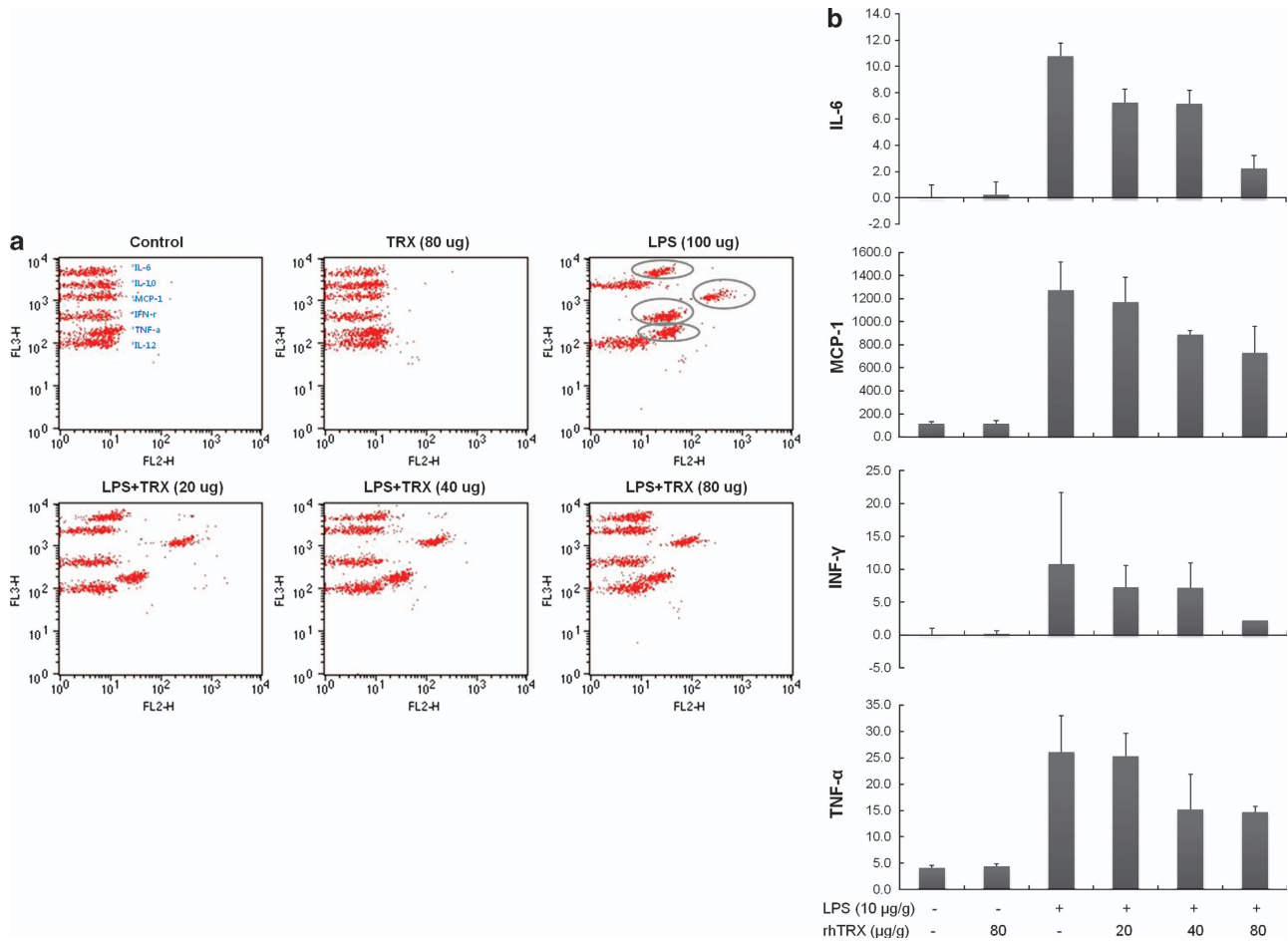


Figure 4 Comparison of inflammatory cytokine levels as determined by CBA (a), represented in concentrations of differentially expressed cytokines (b). C57BL/6 mice were subcutaneously injected with 10 µg of LPS and, after 4 h, with various concentrations of rhTRX. After another 4 h, the levels of IL-6, IL-10, MCP-1, IFN-γ, TNF-α and IL-12 in serum were quantitatively measured by CBA.

intimately associated with lipid metabolism.^{46–49} Accordingly, LPS-downregulated expression of TIP47 and ATP synthase demonstrates that LPS induces inflammation by affecting the inflammatory signaling substances such as ROI and NO, as well as by inducing alterations in lipid metabolism. In the same manner, TRX might exert its protective effects on LPS-stimulated cells at least in part through its ability to modulate a lipid metabolism-dependent pathway by upregulating related proteins such as TIP47 and ATP synthase.^{35–39,50} The effect of TRX on inflammation-related lipid accumulation in the skin was directly verified by the results of Oil Red O staining, which demonstrated that exogenous rhTRX inhibited lipid accumulation after subcutaneous injection of LPS (Figure 3). These results demonstrate that TIP47 and ATP synthase can be considered early markers of a systemic inflammatory reaction in the pathogenesis of skin diseases and associated metabolic syndromes. As a correlation between inflammation and lipid metabolism was observed, development of treatments that selectively target TIP47 and ATP synthase is likely to be effective to slow the progression of inflammatory skin diseases.

The inflammatory response has been reported to be regulated by a variety of cytokines and lipid mediators. Therefore, the design of new drugs to more selectively and completely inhibit cytokines and lipid mediators has emerged as a rational strategy to improve the efficacy of inflammatory disease treatments. The effects of available therapies on the synthesis of inflammatory cytokines and lipid mediators have also been assessed. As a pleiotropic inflammatory cytokine, TNF-α possesses both growth stimulating and inhibitory properties during inflammation. For instance, TNF-α induces not only neutrophil proliferation but also apoptosis upon binding to the TNF-R55 receptor.⁵¹ Previous studies have shown that TNF-α is involved in the modulation of many lipid metabolism-related genes.⁵² It has been also shown that the early stage of the metabolic syndrome is marked by a higher level of TNF-α, which is correlated with changes in lipid metabolism and insulin concentrations.⁵³ Changes in the level of MCP-1 have been also reported to lead to alterations in lipid metabolism. MCP-1 participates in adipogenesis, and its deficiency is known to prevent high-fat-induced obesity.⁵⁴ IL-6 is also involved in lipid metabolism as well as

inflammatory processes.⁵⁵ As depicted in the CBA results (Figure 4), rhTRX dose dependently reduced LPS-stimulated secretion of inflammatory cytokines IL-6, MCP-1, IFN- γ and TNF- α . Considering that IL-6, MCP-1 and TNF- α are potent lipid metabolism regulators in various inflammatory diseases, the results of Figure 4 imply that a correlation among LPS stimulation, lipid accumulation and cytokine secretions exists: LPS exacerbates inflammation at least in part by prompting the secretion of inflammatory cytokines that contribute to disorders of lipid metabolism. These results provide useful information to expand our understanding of how cytokines are regulated in inflammatory responses, which have important implications in the development of effective treatments targeting inflammatory diseases. By contrast, the anti-inflammatory effects of TRX appear to involve decreasing the alterations in lipid metabolism by modulating related cytokines, such as TNF- α , MCP-1, and IL-6. On the basis of the results showing that TRX influences both the expression of TIP47 and ATP synthase and the production of inflammatory cytokines involved in lipid metabolism, further research will be required to support the exciting possibility that a specific correlation exists among TIP47, ATP synthase and those cytokines in the modulation of lipid metabolism during inflammation.

The combined results of this study deepen our understanding of how TRX can protect against inflammatory skin diseases. TRX attenuates inflammation-induced skin cell damage, most likely through decreasing alterations in lipid metabolism by modulating related proteins, such as TIP47 and ATP synthase and cytokines, such as TNF- α , MCP-1 and IL-6. Although further clinical investigations are required to prove the significance and effectiveness of TRX, administration of TRX holds promise as a rational therapeutic strategy to treat inflammation-related disorders of lipid metabolism.

CONFLICT OF INTEREST

The authors declare no conflict of interest.

ACKNOWLEDGEMENTS

We thank Dr Wona Joo for her contribution.

- 1 Thomas M, Peter JV, Williams A, Job V, George R. Systemic inflammatory response syndrome in diseases of the skin. *Postgrad Med J* 2010; **86**: 83–88.
- 2 Torii M, Wang L, Ma N, Saito K, Hori T, Sato-Ueshima M *et al*. Thioredoxin suppresses airway inflammation independently of systemic Th1/Th2 immune modulation. *Eur J Immunol* 2009; **40**: 787–796.
- 3 Fuchs J, Huflejt ME, Rothfuss LM, Wilson DS, Carcamo G, Packer L. Acute effects of near ultraviolet and visible light on the cutaneous antioxidant defense system. *Photochem Photobiol* 1989; **50**: 739–744.
- 4 Fuchs J, Huflejt ME, Rothfuss LM, Wilson DS, Carcamo G, Packer L. Impairment of enzymic and nonenzymic antioxidants in skin by UVB irradiation. *J Invest Dermatol* 1989; **93**: 769–773.
- 5 Shindo Y, Witt E, Han D, Packer L. Dose-response effects of acute ultraviolet irradiation on antioxidants and molecular markers of oxidation in murine epidermis and dermis. *J Invest Dermatol* 1994; **102**: 470–475.
- 6 Peus D, Meves A, Pott M, Beyerle A, Pittelkow MR. Vitamin E analog modulates UVB-induced signaling pathway activation and enhances cell survival. *Free Radic Biol Med* 2001; **30**: 425–432.
- 7 Sato A, Hoshino Y, Hara T, Muro S, Nakamura H, Mishima M *et al*. Thioredoxin-1 ameliorates cigarette smoke-induced lung inflammation and emphysema in mice. *J Pharmacol Exp Ther* 2008; **325**: 380–388.
- 8 Ohashi S, Nishio A, Nakamura H, Kido M, Ueno S, Uza N *et al*. Protective roles of redox-active protein thioredoxin-1 for severe acute pancreatitis. *Am J Physiol* 2006; **290**: G772–G781.
- 9 Bertini R, Howard OM, Dong HF, Oppenheim JJ, Bizzarri C, Sergi R *et al*. Thioredoxin, a redox enzyme released in infection and inflammation, is a unique chemoattractant for neutrophils, monocytes, and T cells. *J Exp Med* 1999; **189**: 1783–1789.
- 10 Shchedrina VA, Novoselov SV, Malinowski MY, Gladyshev VN. Identification and characterization of a selenoprotein family containing a diselenide bond in a redox motif. *Proc Natl Acad Sci USA* 2007; **104**: 13919–13924.
- 11 Arner ES, Holmgren A. Physiological functions of thioredoxin and thioredoxin reductase. *Eur J Biochem* 2000; **267**: 6102–6109.
- 12 Quan S, Schneider I, Pan J, Von Hacht A, Bardwell JC. The CXXC motif is more than a redox rheostat. *J Biol Chem* 2007; **282**: 28823–28833.
- 13 Wiita AP, Perez-Jimenez R, Walther KA, Grater F, Berne BJ, Holmgren A *et al*. Probing the chemistry of thioredoxin catalysis with force. *Nature* 2007; **450**: 124–127.
- 14 Kurimoto C, Kawano S, Tsuji G, Hatachi S, Jikimoto T, Sugiyama D *et al*. Thioredoxin may exert a protective effect against tissue damage caused by oxidative stress in salivary glands of patients with Sjogren's syndrome. *J Rheumatol* 2007; **34**: 2035–2043.
- 15 Toledano MB, Kumar C, Le Moan N, Spector D, Tacnet F. The system biology of thiol redox system in *Escherichia coli* and yeast: differential functions in oxidative stress, iron metabolism and DNA synthesis. *FEBS Lett* 2007; **581**: 3598–3607.
- 16 Chen Y, Cai J, Jones DP. Mitochondrial thioredoxin in regulation of oxidant-induced cell death. *FEBS Lett* 2006; **580**: 6596–6602.
- 17 Holmgren A. Thioredoxin and glutaredoxin systems. *J Biol Chem* 1989; **264**: 13963–13966.
- 18 Young JJ, Patel A, Rai P. Suppression of thioredoxin-1 induces premature senescence in normal human fibroblasts. *Biochem Biophys Res Commun* 2002; **292**: 363–368.
- 19 Sachi Y, Hirota K, Masutani H, Toda K, Okamoto T, Takigawa M *et al*. Induction of ADF/TRX by oxidative stress in keratinocytes and lymphoid cells. *Immunol Lett* 1995; **44**: 189–193.
- 20 Arai RJ, Masutani H, Yodoi J, Debbas V, Laurindo FR, Stern A *et al*. Nitric oxide induces thioredoxin-1 nuclear translocation: possible association with the p21Ras survival pathway. *Biochem Biophys Res Commun* 2006; **348**: 1254–1260.
- 21 Tanito M, Kwon YW, Kondo N, Bai J, Masutani H, Nakamura H *et al*. Cytoprotective effects of geranylgeranylacetone against retinal photooxidative damage. *J Neurosci* 2005; **25**: 2396–2404.
- 22 Liu W, Nakamura H, Shioji K, Tanito M, Oka S, Ahsan MK *et al*. Thioredoxin-1 ameliorates myosin-induced autoimmune myocarditis by suppressing chemokine expressions and leukocyte chemotaxis in mice. *Circulation* 2004; **110**: 1276–1283.
- 23 Jaulmes A, Thierry S, Janvier B, Raymondjean M, Marechal V. Activation of sPLA2-IIA and PGE2 production by high mobility group protein B1 in vascular smooth muscle cells sensitized by IL-1 β . *Faseb J* 2006; **20**: 1727–1729.
- 24 Hyun JW, Jung YC, Kim HS, Choi EY, Kim JE, Yoon BH *et al*. 8-hydroxydeoxyguanosine causes death of human leukemia cells deficient in 8-oxoguanine glycosylase 1 activity by inducing apoptosis. *Mol Cancer Res* 2003; **1**: 290–299.
- 25 Karsan A, Blonder J, Law J, Yaquian E, Lucas DA, Conrads TP *et al*. Proteomic analysis of lipid microdomains from lipopolysaccharide-activated human endothelial cells. *J Proteome Res* 2005; **4**: 349–357.
- 26 Turler A, Schwarz NT, Turler E, Kalff JC, Bauer AJ. MCP-1 causes leukocyte recruitment and subsequently endotoxemic ileus in rat. *Am J Physiol* 2002; **282**: G145–G155.
- 27 Slomiany A, Slomiany BL. Lipidomic processes in homeostatic and LPS-modified cell renewal cycle. Role of phosphatidylinositol 3-kinase pathway in biomembrane synthesis and restitution of apical epithelial membrane. *J Physiol Pharmacol* 2003; **54**: 533–551.
- 28 Cho CW, Lee SH, Choi J, Park SJ, Ha DJ, Kim HJ *et al*. Improvement of the two-dimensional gel electrophoresis analysis for the proteome study of *Halobacterium salinarum*. *Proteomics* 2003; **3**: 2325–2329.
- 29 Bozinovski S, Cross M, Vlahos R, Jones JE, Hsuu K, Tessier PA *et al*. S100A8 chemotactic protein is abundantly increased, but only a minor contributor to LPS-induced, steroid resistant neutrophilic lung inflammation in vivo. *J Proteome Res* 2005; **4**: 136–145.

- 30 Bradford MM. A rapid and sensitive method for the quantitation of microgram quantities of protein utilizing the principle of protein-dye binding. *Anal Biochem* 1976; **72**: 248–254.
- 31 Marchand C, Le Marechal P, Meyer Y, Decottignies P. Comparative proteomic approaches for the isolation of proteins interacting with thioredoxin. *Proteomics* 2006; **6**: 6528–6537.
- 32 Yamamoto K, Yasukawa F, Ito S. Measurement of the sugar-binding specificity of lectins using multiplexed bead-based suspension arrays. *Methods Mol Biol* 2007; **381**: 401–409.
- 33 Ferbas J, Thomas J, Hodgson J, Gaur A, Casadevall N, Swanson SJ. Feasibility of a multiplex flow cytometric bead immunoassay for detection of anti-epoetin alfa antibodies. *Clin Vaccine Immunol* 2007; **14**: 1165–1172.
- 34 Brasaemle DL. The perilipin family of structural lipid droplet proteins: Stabilization of lipid droplets and control of lipolysis. *J Lipid Res* 2007; **48**: 2547–2559.
- 35 Tsuiki E, Fujita A, Ohsaki Y, Cheng J, Irie T, Yoshikawa K *et al*. All-trans-retinol generated by rhodopsin photobleaching induces rapid recruitment of TIP47 to lipid droplets in the retinal pigment epithelium. *Invest Ophthalmol Vis Sci* 2007; **48**: 2858–2867.
- 36 Russell TD, Palmer CA, Orlicky DJ, Fischer A, Rudolph MC, Neville MC *et al*. Cytoplasmic lipid droplet accumulation in developing mammary epithelial cells: roles of adipophilin and lipid metabolism. *J Lipid Res* 2007; **48**: 1463–1475.
- 37 Turro S, Ingelmo-Torres M, Estanyol JM, Tebar F, Fernandez MA, Albor CV *et al*. Identification and characterization of associated with lipid droplet protein 1: a novel membrane-associated protein that resides on hepatic lipid droplets. *Traffic* 2006; **7**: 1254–1269.
- 38 Sztalryd C, Bell M, Lu X, Mertz P, Hickenbottom S, Chang BH *et al*. Functional compensation for adipose differentiation-related protein (ADFP) by Tip47 in an ADFP null embryonic cell line. *J Biol Chem* 2006; **281**: 34341–34348.
- 39 Ljung L, Olsson T, Engstrand S, Wallberg-Jonsson S, Soderberg S, Rantapaa-Dahlqvist S. Interleukin-1 receptor antagonist is associated with both lipid metabolism and inflammation in rheumatoid arthritis. *Clin Exp Rheumatol* 2007; **25**: 617–620.
- 40 Kubala L, Schmelzer KR, Klinke A, Kolarova H, Baldus S, Hammock BD *et al*. Modulation of arachidonic and linoleic acid metabolites in myeloperoxidase-deficient mice during acute inflammation. *Free Radic Biol Med* 2010; **48**: 1311–1320.
- 41 Filep JG. Lipid mediator interplay: resolvin D1 attenuates inflammation evoked by glutathione-conjugated lipid peroxidation products. *Br J Pharmacol* 2009; **158**: 1059–1061.
- 42 Posey KA, Clegg DJ, Printz RL, Byun J, Morton GJ, Vivekanandan-Giri A *et al*. Hypothalamic proinflammatory lipid accumulation, inflammation, and insulin resistance in rats fed a high-fat diet. *Am J Physiol Endocrinol Metab* 2009; **296**: E1003–E1012.
- 43 Robenek H, Robenek MJ, Buers I, Lorkowski S, Hofnagel O, Troyer D *et al*. Lipid droplets gain PAT family proteins by interaction with specialized plasma membrane domains. *J Biol Chem* 2005; **280**: 26330–26338.
- 44 Bulankina AV, Deggerich A, Wenzel D, Mutenda K, Wittmann JG, Rudolph MG *et al*. TIP47 functions in the biogenesis of lipid droplets. *J Cell Biol* 2009; **185**: 641–655.
- 45 Bell M, Wang H, Chen H, McLenithan JC, Gong DW, Yang RZ *et al*. Consequences of lipid droplet coat protein downregulation in liver cells: abnormal lipid droplet metabolism and induction of insulin resistance. *Diabetes* 2008; **57**: 2037–2045.
- 46 Bae TJ, Kim MS, Kim JW, Kim BW, Choo HJ, Lee JW *et al*. Lipid raft proteome reveals ATP synthase complex in the cell surface. *Proteomics* 2004; **4**: 3536–3548.
- 47 Marcet B, Libert F, Boeynaems JM, Communi D. Extracellular nucleotides induce COX-2 up-regulation and prostaglandin E2 production in human A549 alveolar type II epithelial cells. *Eur J Pharmacol* 2007; **566**: 167–171.
- 48 Brehm A, Krssak M, Schmid AI, Nowotny P, Waldhausl W, Roden M. Increased lipid availability impairs insulin-stimulated ATP synthesis in human skeletal muscle. *Diabetes* 2006; **55**: 136–140.
- 49 Champagne E, Martinez LO, Collet X, Barbaras R. Ecto-F1Fo ATP synthase/F1 ATPase: metabolic and immunological functions. *Curr Opin Lipidol* 2006; **17**: 279–284.
- 50 Brasaemle DL. Thematic review series: adipocyte biology. The perilipin family of structural lipid droplet proteins: stabilization of lipid droplets and control of lipolysis. *J Lipid Res* 2007; **48**: 2547–2559.
- 51 Murray J, Barbara JA, Dunkley SA, Lopez AF, Van Ostade X, Condliffe AM *et al*. Regulation of neutrophil apoptosis by tumor necrosis factor- α : requirement for TNFR55 and TNFR75 for induction of apoptosis in vitro. *Blood* 1997; **90**: 2772–2783.
- 52 Tai CC, Ding ST. N-3 polyunsaturated fatty acids regulate lipid metabolism through several inflammation mediators: mechanisms and implications for obesity prevention. *J Nutr Biochem* 2010; **21**: 357–363.
- 53 Lubitskaia NS, Antoniuk MV, Veremchuk LV, Khodosova KK. Role of tumor necrosis factor in the development of metabolic syndrome. *Terapevticheskie arkhiv* 2009; **81**: 59–63.
- 54 Younce CW, Azfer A, Kolattukudy PE. MCP-1 (monocyte chemoattractant protein-1)-induced protein, a recently identified zinc finger protein, induces adipogenesis in 3T3-L1 pre-adipocytes without peroxisome proliferator-activated receptor gamma. *J Biol Chem* 2009; **284**: 27620–27628.
- 55 Guzman-Guzman IP, Munoz-Valle JF, Flores-Alfaro E, Salgado-Goytia L, Salgado-Bernabe AB, Parra-Rojas I. Interleukin-6 gene promoter polymorphisms and cardiovascular risk factors. a family study. *Disease markers* 2008; **28**: 29–36.



This work is licensed under a Creative Commons Attribution 3.0 Unported License. To view a copy of this license, visit <http://creativecommons.org/licenses/by/3.0/>